Magnetization dynamics and relaxation in epitaxial FePd thin films with a stripe domain structure

N. Vukadinovic[1,a], H. Le Gall[2], J. Ben Youssef[2] V. Gehanno[3], A. Marty[3], Y. Samson[3], and B. Gilles[4]

[1] Dassault Aviation, 92552 Saint-Cloud, France
[2] Laboratoire de Physique du Solide de Bellevue, CNRS, 92195 Meudon, France
[3] CEA-Grenoble, Département de Recherche Fondamentale sur la Matière Condensée/SP2M, 17 rue des Martyrs, 38054 Grenoble Cedex 9, France
[4] LTPCM, ENSEEG, B.P.75, 38042 Grenoble, France

Abstract. FMR investigations on epitaxial partially ordered FePd thin films with a perpendicular magnetic anisotropy (PMA) are presented. The measurements have been performed over a wide frequency range (6–18 GHz) in the multidomain state where a weak-stripe domain structure exists. Parallel FMR measurements exhibit three magnetic excitations. Their dispersion curves, frequency *versus* resonance field, and the frequency dependence of the related resonance linewidths are reported. It is shown that the resonance fields and linewidths increase with frequency. For the two main modes identified with domain modes, these behaviors are correctly described by the Domain Mode Ferromagnetic Resonance (DM-FMR) model. Especially, the DM-FMR field-swept linewidth expressions assuming a Landau-Lifshitz-Gilbert-type relaxation have been derived and compared satisfactorily with the experimental data. The physical origin of the third excitation is discussed in terms of domain wall and spin-wave modes.

PACS. 76.50.+g Ferromagnetic, antiferromagnetic, and ferrimagnetic resonances; spin-wave resonance – 75.50.-i Studies of specific magnetic materials – 75.30.Kz Magnetic phase boundaries (including magnetic transitions, metamagnetism, etc.)

1 Introduction

In the recent past years, continuing interest in spin dynamics of unsaturated ferromagnetic thin films has been motivated by the observation of new resonance modes [1–4]. These modes have been investigated by means of two common experimental methods: measurements of microwave initial permeability and Ferromagnetic Resonance (FMR) experiments. Concerning the former technique, the existence of multiple narrow resonances in frequency permeability spectra has been reported in amorphous Co-Nb-Zr [1] and Co-Fe-Zr [2] thin films exhibiting a weak PMA. These excitations have been attributed to domain modes and spin-wave modes [1,2]. In both cases, the occurrence of multiple resonances is closely related to the presence of fine stripe domains (weak-stripe type) with an aspect ratio $P_0/t \sim 1$ (P_0 is the stripe period, and t is the film thickness).

Concerning the FMR technique, Ebels *et al.* [3,4] described recently FMR experiments for perpendicularly magnetized Co (0001) thin films supporting a nanoscale strong stripe-domain structure with $P_0/t \sim 2$.

Complicated FMR spectra with a series of modes have been also observed.

In this present work, we report wide band (6–18 GHz) FMR experiments on a FePd thin film having a moderate PMA. Indeed, such a film with an in-plane easy axis but also a PMA may exhibit spontaneously a parallel stripe domain configuration. The experimental data are analyzed from the DM-FMR model [5] as a first approach.

2 Sample preparation and magnetometry

The sample was prepared using Molecular Beam Epitaxy under Ultra-High vacuum (10^{-7} Pa). A 2 nm seed layer of Cr was deposited onto a MgO (001)-oriented single crystal substrate in order to allow the epitaxial growth of a 60 nm single crystal Pd buffer layer. After 10 minutes annealing at 700 K, a 50 nm thick FePd alloy layer having the (001) growth direction was deposited at room temperature using a mono-layer (ML) by mono-layer growth method in order to induce a chemical order similar to the one found in the tetragonal structure $L1_0$ [6,7]. The multilayer $(Fe_{1ML}Pd_{1ML})_{130}$ was then capped with a 2 nm thick Pd layer in order to prevent oxidation. A detailed

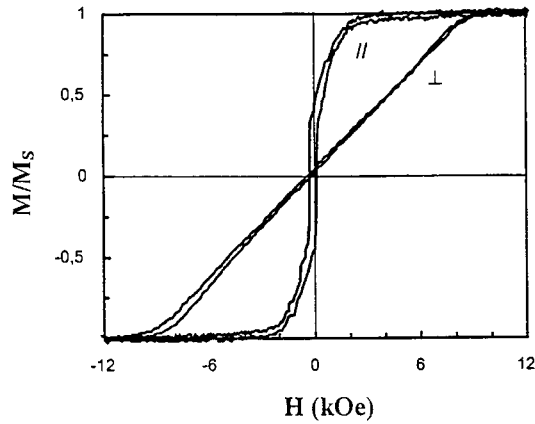[a] e-mail: `nicolas.vukadinovic@dassault.aviation.fr`

Fig. 1. The normalized magnetization component parallel with the applied magnetic field, M/M_s, *vs.* applied magnetic field. (//) field applied in the specimen plane, M/M_s measured using a vibrating sample magnetometer. ($\perp$) field applied perpendicular to the specimen plane, M/M_s measured using the polar Kerr effect.

study of the structure of the sample using X-ray diffraction and EXAFS is reported elsewhere [8]. These investigations have shown the existence of a weak long range order and a large directional short range order, corresponding to an anisotropy of the chemical order in the first coordination shell. Due to this structural anisotropy, a magnetocrystalline anisotropy is expected.

The magnetization curves were measured using a vibrating sample magnetometer (VSM) for the in-plane measurements and using polar Kerr effect magnetometer for a perpendicular applied magnetic field. The normalized curves $M/M_s(H)$ presented in Figure 1 reveal that the easy axis of the sample lies in the plane of the layers. The saturation magnetization and the uniaxial anisotropy constant associated with the PMA were both estimated from VSM measurements: $M_s = 1050\,(\pm 15\%)$ emu/cm^3 and $K_u = 2.6 \times 10^6\,(\pm 25\%)$ erg/cm^3. The value of the uniaxial anisotropy constant has also been extracted from FMR measurements performed in the saturated state [9] together with the gyromagnetic ratio γ giving $K_U = 2.14 \times 10^6$ erg/cm^3 (in good agreement with the VSM results) and $\gamma = 1.85 \times 10^7$ s^{-1}Oe^{-1}. The above value of K_u leads to a quality factor, $Q = 0.4 \pm 0.1$ ($Q = K_U/2\pi M_S^2$). In this kind of material having a weak PMA the so-called weak-stripe structure [10] appears only above a critical thickness h_c: for $h < h_c$ the magnetization lies in the plane of the layer, while for $h > h_c$, an instability of the magnetization gives rise to periodic undulations of the magnetization vector out of the plane of the layers. For a quality factor of about 0.4, it has been shown experimentally that the critical thickness is about 30 nm [11].

The occurrence of a stripe structure has been checked by MFM and the results is shown in Figure 2. The measurements were performed using a Nanoscope IIIa from Digital Instruments, using the ac mode. The images demonstrate clearly the existence of a well-organized periodic stripe structure. The period has been estimated to
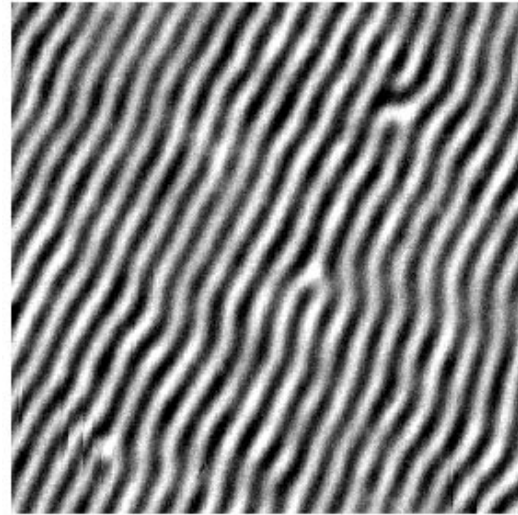

Fig. 2. 2 μm $\times$ 2 μm zero-field MFM image showing nearly periodic parallel stripes. The stripes are aligned along the direction of the last applied dc magnetic field within the plane of the sample. The film thickness is 50 nm and the period has been estimated to be 107 nm.

be 107 nm from a Power spectrum density analysis on a larger image in order to improve the statistics. The weak-stripe character of this magnetic structure has also been confirmed by Mössbauer measurements [12] on the same sample.

3 FMR in the unsaturated state

A previous FMR study in the saturated state on the same sample has been reported in reference [9]. In this section, the parallel FMR with an applied dc field $H^{//}$, less than the parallel saturation field $H_S^{//}$, and oriented along the stripe direction is considered. FMR experiments were conducted over the frequency range 6–18 GHz using a highly sensitive wide band resonance spectrometer with non-resonant microstrip transmission line [13].

3.1 A brief review of magnetic excitations of a stripe-domain structure

Firstly, it is fruitful to refer to the many works devoted to magnetic excitations in garnet films having a perpendicular magnetic anisotropy supporting parallel stripe domains. It is well-established that mainly two types of magnetic excitations can exist in such a magnetic structure: (i) Domain Mode Ferromagnetic Resonance (DM-FMR) which corresponds to FMR within the domains [14]. These modes are mainly excited by an rf magnetic field h_{rf} in the film plane. The stripe symmetry permits two DM-FMR modes which are called ω^- and

ω^+ according to Artman's notation [15]. In the presence of an applied dc field $H^{//}$ along the stripe direction, the ω^- or optic mode is excited by the component of h_{rf} parallel to $H^{//}$ and the ω^+ or acoustic mode by the component of h_{rf} perpendicular to $H^{//}$; (ii) Domain Wall Resonances (DWR) which correspond to collective modes of domain wall vibrations [16,17]. These modes are excited by h_{rf} parallel to the easy axis of magnetization. From these previous studies, some results concerning DM-FMR and DWR can be reviewed: (i) The slope of the dispersion curve, frequency *versus* $H_R^{//}$, $H_R^{//}$ is the parallel resonance field, strongly depends on the Q-factor for the ω^+ mode. For magnetic garnet films with high Q-values ($Q > 1$), $H_R^{//}$ decreases as the frequency increases [5]. For intermediate Q-values ($Q \sim 0.5-1$) $H_R^{//}$ is found to be nearly constant with frequency [18,19]. For low Q-values ($Q \sim 0.2$), $H_R^{//}$ increases with frequency [20]. The parallel FMR is observed as a continuation of the ω^+ mode. The ω^- resonance field decreases as frequency increases for these data with $Q \geq 0.2$. (ii) The DWR fields increase with frequency for the reported data with $Q \geq 0.6$ [18,19,21,22]. In addition, for high and intermediate Q-values, the fundamental DWR occurs at lower frequency than the DM-FMR [18,19]. In contrast, for low Q-values the fundamental DWR is observed at higher frequency than the DM-FMR [20]. (iii) These experimental behaviors have been analyzed by using the extended Smit and Beljers model [23] (denoted DM-FMR model) for the DM-FMR modes, the well-known harmonic oscillator model [24] for the fundamental DWR mode or a hybridization of these two models [5,19]. Although, these models assume a large Q-factor and are based on the existence of perpendicular alternatively up and down stripe domains with magnetization constant within the domains, a satisfactory description of experimental evolutions is found for intermediate [18,19] and sometimes even for low-Q values [20].

By neglecting the coupling between the DM-FMR and DWR modes, the DM-FMR resonance conditions for the ω^- and ω^+ modes in the presence of $H^{//}$ are given respectively by [5]:

$$\Omega^2 = (1-p)(1+2(r-p))\left(1 - \frac{h_-{}^2}{(1-p)^2}\right), \quad (1)$$

and

$$\Omega^2 = (1-p)\left(1 - p + \frac{h_+^2}{(1-p)^2}(2r-1)\right), \quad (2)$$

where $\Omega = \frac{\omega}{4\pi\gamma M_S Q}$, $p = \frac{N_{ZZ}}{Q}$, $r = \frac{1}{2Q}$, $h_{-/+} = \frac{H_{R,-/+}^{//}}{4\pi M_S Q}$, with $H_{R,-}^{//}$ (resp. $H_{R,+}^{//}$) is the resonance field for the ω^- mode (resp. ω^+ mode).
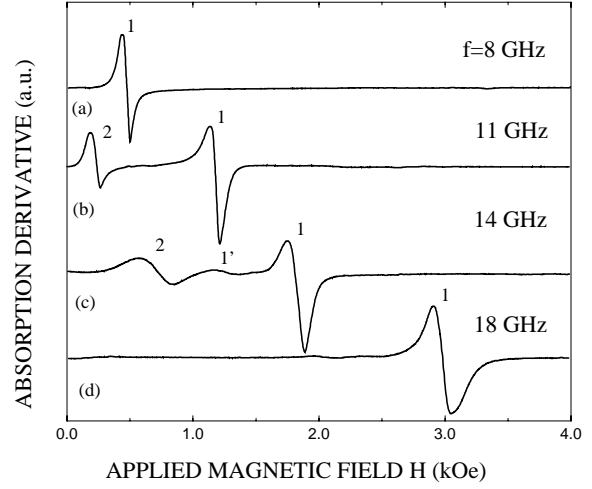

Fig. 3. Experimental FMR derivative spectra: (a) $f = 8$ GHz; (b) $f = 11$ GHz; (c) $f = 14$ GHz, (d) $f = 18$ GHz. The applied dc magnetic field is along the stripe direction.

The demagnetization factor N_{ZZ} $(H^{//})$ is related to the stripe period P_0 $(H^{//})$ by the relation [25]:

$$N_{ZZ}(H^{//}) = \frac{32}{\pi^2}\frac{P_0(H^{//})}{t}\sum_{odd}^{\infty}\frac{1}{n^3}\frac{\sinh(V)}{\sinh(V)+\sqrt{\mu}\cosh(V)}, \quad (3)$$

where $V = \frac{\pi n t \sqrt{\mu}}{P_0}$, t is the film thickness, and $\mu \approx 1 + 1/Q$ is the rotational permeability. In the usual calculations of DM-FMR for high-Q materials, $P_0(H^{//})$ is computed following the procedure of Druyvesteyn *et al.* [26].

The resonance condition for the fundamental DWR mode in the presence of $H^{//}$ deduced from the harmonic oscillator model is defined by [5]:

$$\omega = \sqrt{\frac{k}{m}}, \quad (4)$$

where $k(H^{//})$ is the restoring force and $m(H^{//})$ is the domain wall mass.

3.2 Experimental results and discussion

3.2.1 Dispersion curves

Figure 3 reports FMR derivative spectra recorded respectively at 8, 11, 14 and 18 GHz in the presence of an applied planar dc magnetic field $H^{//}$ parallel to the direction of stripe domains. For frequencies lower than 10 GHz, one mode (designated 1) is observed (curve (a)). For frequencies ranging from 10 to 16 GHz, a second mode (designated 2) of weaker intensity than the first one appears (curve (b)). The location of these two resonance lines
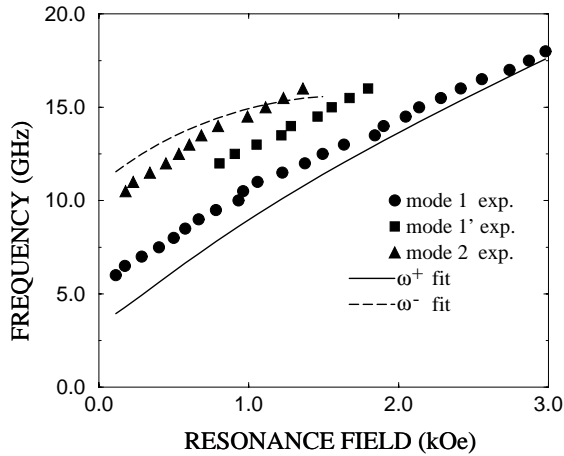
Fig. 4. In-plane dispersion curves for the three observed excitations. Experimental data are denoted by symbols; mode 1 (circles), mode 1' (squares) and mode 2 (triangles). The theoretical fits are represented by a solid line (ω^+ mode) and a dashed line (ω^- mode).
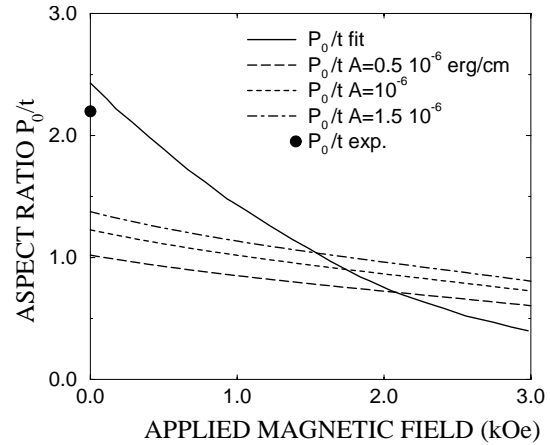
Fig. 5. Variation of the aspect ratio P_0/t as a function of the applied dc magnetic field along the stripe direction. The best profile P_0^{fit}/t corresponding to the data of Figure 4 is given by the solid line. The dashed lines represent the evolutions of P_0/t deduced from the Druyvesteyn's model (high Q-limit) for three values of A.

shifts towards higher fields with increasing frequency. Furthermore, the linewidth of this second resonance peak increases rapidly with frequency (curve (c)). Consequently, this mode becomes difficult to observe above 16 GHz. It is worth noting the existence of a subsidiary mode (designated 1') located between the two main modes. This peak is clearly observed in the reduced 12–16 GHz range (curve (c)). For frequencies greater than 16 GHz, only the mode 1 is clearly observed which merges into the uniform parallel FMR at 18 GHz where the resonance field exceeds the parallel saturation field (curve (d)). The dispersion curves of frequency *versus* the parallel resonance field for the three excitations is shown in Figure 4. Since for our film $Q \sim 0.4$, it is tempting to use the concept of DM-FMR and DWR as a first approach. From the discussion of Section 3.1., it seems reasonable to identify the mode 1 with ω^+. In order to determine the nature of modes 1' and 2, the DM-FMR conditions (Eqs. (1, 2)) have been computed. However, to account for the discrepancy, as it may be seen below in Figure 5, between the experimental value of P_0/t at zero field and the theoretical one deduced from the Druyvesteyn's model, we decided to consider P_0 as a free parameter. The best fit is reported in Figure 4. It appears that the experimental dispersion curves of the modes 1 and 2 are correctly described by the DM-FMR theory. The above results suggest that one identify the mode 2 with ω^-. Nevertheless, the gap between the modes 1 and 2 are overestimated by the theory. The best fit obtained from the data for $P_0^{\text{fit}}(H^{//})/t$ is plotted in Figure 5 and compared with those computed by the Druyvesteyn procedure for three realistic values of A; 5×10^{-7}, 1×10^{-6} and 1.5×10^{-6} erg/cm. It is noted that P_0^{fit}/t decreases more rapidly with increasing $H^{//}$ than the three straightforward calculated profiles. Such a variation of P_0^{fit}/t reflects the existence of an important distortion of the domain structure with respect to the idealistic parallel stripe do-

mains considered in the DM-FMR theory. As expected for a relatively low-Q material, the probable presence of closure domains, the presumed non-uniformity of the magnetization inside the domains and the existence of non-vanishing thickness domain walls with a complex internal structure could explain this behavior.

Concerning the mode 1', two interpretations can be advanced. First, according to reference [4], the mode 1' could be attributed to the fundamental DWR. Although, the evaluation of the resonance condition (Eq. (4)) taking into account the profile $P_0^{\text{fit}}(H^{//})/t$ yields the presence of DWR beyond 15 GHz, this calculation is based on the hypothesis of a pure Bloch-wall. In low-Q materials supporting a weak-stripe domain structure a more complicated domain wall structure is expected which can deeply modify the DWR dispersion curve. Second, the existence of a spin-wave mode with an optic character [3] could also be proposed. Indeed, the experimental field separations δH_{exp} between the modes 1 and 1' appear approximately independent of frequency and $\delta H_{\text{exp}} \approx 600$ Oe. The theoretical field separations calculated by assuming the existence of spin-wave modes quantized across the film thickness as well as the domain width $P_0/2$ is given by [3]:

$$\delta H_{(n,m)-(n',m')} = \frac{2A}{M_S}\pi^2\left(\frac{n'^2 - n^2}{t^2} + \frac{4}{P_0^2}(m'^2 - m^2)\right), \tag{5}$$

where (n, m) and (n', m') are the mode numbers, n, m, n', m' odd integers. Assigning the mode $(1,1)$ to the peak 1 and taking $A = 10^{-6}$ erg/cm, $t = 50$ nm and $P_0/2 = 53.5$ nm (the largest value, $P_0 = P_0(H^{//} = 0)$) this leads to $\delta H_{(1,1)-(n',m')} > 5000$ Oe whatever are n' and m', much larger than the experimental shift
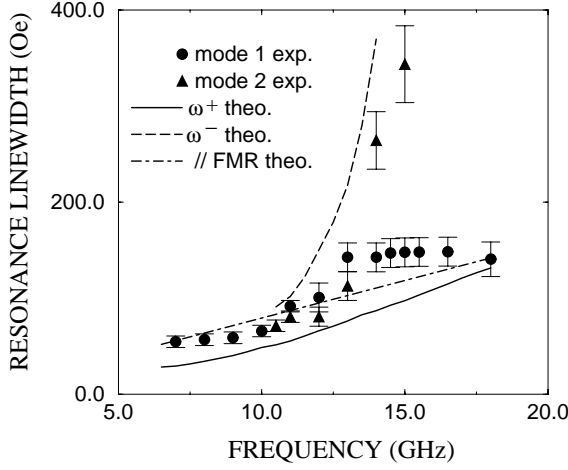
Fig. 6. Peak-to-peak linewidths of the two main excitations as a function of frequency. Experimental data are denoted by symbols; mode 1 (circles), and mode 2 (triangles). The theoretical parallel FMR linewidth $\Delta H_{p-p}^{//} = \frac{2\alpha\omega}{\sqrt{3}\gamma}$ (saturated state) is indicated by a dot-dashed line. The theoretical DM-FMR linewidths assuming a Gilbert type of relaxation are represented by a solid line (ω^+ mode) and a dashed line (ω^- mode). α is equal to 2×10^{-2}.

$\delta H_{\mathrm{exp}} \approx 600$ Oe. Solely by indexing the peak 1 as the fundamental mode $(0,0)$ and the peak $1'$ as the mode $(1,0)$, we obtain $\delta H_{(0,0)-(1,0)} \approx 750$ Oe which is of the same order of magnitude as δH_{exp}. Further investigations are needed to confirm either interpretation.

3.2.2 Linewidths

The evolutions of peak-to-peak resonance linewidths for the two main modes as a function of frequency are displayed in Figure 6. In both cases, an increase of resonance linewidths with frequency is observed. Nevertheless, a saturation of the resonance linewidth is noted for the mode 1 beyond 14 GHz while the resonance linewidth of the mode 2 continues to increase rapidly. First, it is instructive to compare these experimental behaviors with the theoretical evolution predicted by the Gilbert form of relaxation by assuming the sample in the saturated state. In this case, the theoretical peak-to-peak parallel FMR linewidth $\Delta H_{p-p}^{//}$ presents a linear evolution *versus* frequency [27]: $\Delta H_{p-p}^{//} = \frac{2\alpha\omega}{\sqrt{3}\gamma}$, where α is the Gilbert damping parameter, and assuming a Lorentzian shaped absorption curve. This evolution computed with the value $\alpha = 2 \times 10^{-2}$ deduced from the experimental $\Delta H_{p-p}^{//}$ at 18 GHz where the sample is really saturated is indicated in Figure 6. It is observed that the amplitude of variation of $\Delta H_{p-p}^{//}$ is close to the one of the mode 1. Second, the effect of the stripe domain is considered under the approximation of the DM-FMR theory. By introducing the damping parameter α in the DM-FMR theory, the frequency-swept linewidths for

the modes ω^- and ω^+ are given respectively by:

$$\Delta\Omega_- = \alpha\left[2(1+r) - 3p - \frac{h_-^2}{1-p}\right], \qquad (6)$$

$$\Delta\Omega_+ = \alpha\left[2(1-p) + \frac{h_+^2}{(1-p)^2}(2r-1)\right]. \qquad (7)$$

The frequency-swept linewidths can be converted to field-swept linewidths by using the relationship: $\Delta h = \frac{\partial h}{\partial\Omega}\Delta\Omega$ valid for $\Omega \gg \Delta\Omega$. One obtains the following expressions:

$$\Delta h_\pm = 2\Omega\frac{\Delta\Omega_\pm}{D_\pm}, \qquad (8)$$

where

$$D_- = -\frac{\mathrm{d}p}{\mathrm{d}h}\left[3 + 2r - 4p + \frac{(2r-1)}{(1-p)^2}h_-^2\right]$$
$$- \frac{2h_-}{1-p}(1 + 2(r-p)),$$

$$D_+ = \frac{\mathrm{d}p}{\mathrm{d}h}\left[-2(1-p) + \frac{(2r-1)}{(1-p)^2}h_+^2\right] + \frac{2h_+}{1-p}(2r-1),$$

and the parameters p, h, r are defined according to equation (2).

The theoretical curves $\Delta H_{p-p,-}^{//}$ and $\Delta H_{p-p,+}^{//}$ ($\Delta H_{p-p,\pm}^{//} = \Delta h_\pm 4\pi M_S Q/\sqrt{3}$) are plotted in Figure 6. The slope $\mathrm{d}p/\mathrm{d}h$ is computed from the profile $P_0^{\mathrm{fit}}(H^{//})/t$ reported in Figure 5 and $\alpha = 2 \times 10^{-2}$. As a result, the DM-FMR theory including the α-type relaxation formalism reproduces correctly the increase of resonance linewidths with frequency, in particular the rapid variation of the mode 2. It is worth noting that the frequency dependence of $\Delta H_{p-p,+}^{//}$ is close to the one of $\Delta H_{p-p}^{//}$ obtained by assuming the sample in the saturated state. The quantitative discrepancies between the experimental and theoretical linewidths are probably due in part to the discrepancies between the experimental and theoretical dispersion curves (Fig. 4). This comparison seems to confirm the assignment of the modes 1 and 2 to DM-FMR modes. However, the observed saturation of the resonance linewidth for the ω^+ mode is not explained by the model. Concerning the mode $1'$, the determination of the resonance linewidth is less accurate due to the weak intensity of the signal. Typically, $\Delta H_{p-p,1'}^{//} = (190 \pm 40)$ Oe at 14 GHz, and an increase of $\Delta H_{p-p,1'}^{//}$ with frequency of comparable rate to the one of the peak 2 seems to exist.

4 Conclusion

In this work, magnetization dynamics and relaxation in epitaxial FePd thin films with a perpendicular anisotropy have been investigated in the frequency range 6–18 GHz.

FMR measurements in the multidomain state have revealed the existence of three magnetic excitations.

The simple DM-FMR model allows us to reproduce satisfactorily the frequency dependence of the two main modes (mode positions and linewidths), thus confirming the proposed attribution of these lines. In particular, the frequency evolution of linewidths is correctly described by the expressions of DM-FMR linewidths that have been established using the Landau-Lifshitz-Gilbert relaxation term.

This first approach has been chosen due to the lack of precise informations on the real magnetic domain structure. Further investigations by means of analytical models and numerical micromagnetic simulations are in progress to improve our knowledge of the static magnetization distribution. In addition, two possible attributions (domain wall or spin wave) have been advanced for the third observed mode. However, its physical origin is not yet clear. From an experimental point of view, FMR studies in FePd thin films with different Q-values would be of a great interest especially for interpreting the third mode and confirming either interpretation

References

1. Y. Shimada, M. Shimoda, O. Kitakami, Jpn J. Appl. Phys. **34**, 4786 (1995).
2. O. Acher, C. Boscher, B. Brulé, G. Perrin, N. Vukadinovic, G. Suran, H. Joinsten, J. Appl. Phys. **81**, 4057 (1997).
3. U. Ebels, P.E. Wigen, K. Ounadjela, J. Magn. Magn. Mater. **177-181**, 1239 (1998).
4. U. Ebels, P.E. Wigen, K. Ounadjela, Europhys. Lett. **46**, 94 (1999).
5. M. Ramesh, P.E. Wigen, J. Magn. Magn. Mater. **74**, 123 (1988).
6. V. Gehanno, A. Marty, B. Gilles, Y. Samson, Phys. Rev. B **55**, 12552 (1997).
7. V. Gehanno, Y. Samson, A. Marty, B. Gilles, A. Chamberod, J. Magn. Magn. Mater. **172**, 26 (1997).
8. V. Gehanno, C. Revevant-Brizard, A. Marty, B. Gilles, J. Appl. Phys. **84**, 2316 (1998).
9. J. Ben Youssef, H. Le Gall, N. Vukadinovic, V. Gehanno, A. Marty, Y. Samson, B. Gilles J. Magn. Magn. Mater. **202**, 277 (1999).
10. A.L. Sukstanskii, K.I. Primak, J. Magn. Magn. Mater. **169**, 31 (1997).
11. V. Gehanno, R. Hoffmann, Y. Samson, A. Marty, S. Auffret, Eur. Phys. J. B **10**, 457 (1999).
12. V. Gehanno, P. Auric, A. Marty, B. Gilles, J. Magn. Magn. Mater. **188**, 310 (1998).
13. H. Le Gall, N. Vukadinovic, IEEE Trans Magn. **MAG-24**, 3051 (1988).
14. D. Polder, J. Smit, Rev. Mod. Phys. **25**, 89 (1953).
15. J.O. Artman, Phys. Rev. **105**, 74 (1957).
16. J.C. Slonczewski, J. Magn. Magn. Mater. **23**, 305 (1981).
17. N. Vukadinovic, A. Serraj, H. Le Gall, J. Ben Youssef, Phys. Rev. B **58** 385 (1998), and references therein.
18. M. Ramesh, L. Püst, P.E. Wigen, J. Magn. Magn. Mater. **54**, 1205 (1986).
19. B. Lührmann, H. Dötsch, S. Süre, Appl. Phys. A **57**, 553 (1993).
20. M. Ramesh, E.W. Ren, J.O. Artman, M.H. Kryder, J. Appl. Phys. **64**, 5483 (1988).
21. S. Batra, P.E. Wigen, J. Appl. Phys. **61**, 4207 (1987).
22. H. Le Gall, N. Vukadinovic, J. Ostorero, J.M. Desvignes, J. Magn. Magn. Mater. **84**, 229 (1990).
23. J.O Artman, S.H. Charap, J. Appl. Phys. **49**, 1587 (1978).
24. J. Morkowski, H. Dötsch, P.E. Wigen, R.J. Yeh, J. Magn. Magn. Mater. **25**, 39 (1981).
25. C. Kooy, U. Enz, Philips Res. Rep. **15**, 7 (1960).
26. W.F. Druyvesteyn, J.W.F. Dorleijn, P.J. Rijnierse, J. Appl. Phys. **44**, 2397 (1973).
27. W. Platow, A.N. Anisimov, G.L. Dunifer, M. Farle, K. Baberschke, Phys. Rev. B **58**, 5611 (1998).